

Underplating Below the Western Chugach Mountains in the Southern Alaska Block Syntaxial Core Constrained by Low-Temperature Thermochronology*

Sean M. Hartman¹, Phillip A. Armstrong¹, and Jeanette C. Arkle¹

Search and Discovery Article #30250 (2012)**

Posted September 17, 2012

*Adapted from oral presentation at AAPG Annual Convention and Exhibition, Long Beach, California, April 22-25, 2012

**AAPG © 2012 Serial rights given by author. For all other rights contact author directly.

¹Geological Sciences, California State University Fullerton, Fullerton, CA (smhartma@usc.edu)

Abstract

Flat-slab subduction of the Yakutat microplate beneath south-central Alaska has played an instrumental role in the deformation of the overlying Southern Alaska Block (SAB). Terrains of the SAB are bound by arcuate fault systems that delineate regions of transpression and compression. North-verging accretion of these terrains form a prominent orogenic chain along Alaska's southern coast, comprised of the Chugach, St. Elias Mountains, and adjacent coastal regions of the Prince William Sound (PWS). Results from several low-temperature thermochronology studies show that focused exhumation is constrained to a few main regions in southern Alaska - these are mainly in the St. Elias region of southeast Alaska where collisional processes cause rapid rock uplift and in the western Chugach Mountains where underplating along the megathrust is interpreted to cause localized rock uplift. However, the localized rock uplift in the western Chugach is inferred from PWS sea level thermochronology age trends that are projected north into the high elevation, glaciated regions of the western Chugach Mountain syntaxial core where age constraints were previously lacking.

Six new apatite (U-Th)/He (AHe) ages were determined from samples in the rugged core of the syntaxial region to evaluate spatial patterns of rock uplift. Ages along a NNW transect from Harvard Glacier to Mt. Sergeant Robinson range from 6.6 ± 0.9 to 10.8 ± 1.6 Ma. Ages along an ENE transect from Inner Lake George to west of Mt. Marcus Baker range from 4.7 ± 0.9 to 7.6 ± 1.4 Ma. However, when these ages are corrected for topographic effects and projected to sea level for comparison with previous sea level ages, their sea level age range is 2 to 6 Ma, with average age 4.1 Ma. The topographically-corrected sea level ages generally decrease into the core of the range where elevations are greatest. Inferred exhumation rates range from 0.3 to 0.5 km/Ma across the syntaxial core; these exhumation rates are the same as rates determined for PWS fiord samples to the south and suggest that late Miocene to recent average exhumation rates have been spatially constant across the region between the terrain-bounding Contact and Border Ranges fault systems. The consistency of the sea level projected

ages and inferred exhumation rates across the syntaxial core supports a kinematic pattern of uniform rock uplift caused predominantly by underplating rather than crustal shortening between the terrain-bounding faults.

References

Brandon, M.T., J.I. Garver, M.K. Roden-Tice, 1998, Late Cenozoic exhumation of the Cascadia accretionary wedge in the Olympic Mountains, northwest Washington State: GSA Bulletin, v. 110/8, p. 985-1009.

Buscher, J.T., A.L. Berger, and J.A. Spotila, 2008, Exhumation in the Chugach-Kenai Mountains belt above the Aleutian subduction zone, southern Alaska, in J.T. Freymueller, P.J. Haeussler, R.J. Esson, and G. Ekstrom, (eds.), Active tectonics and seismic potential of Alaska: Geophysical Monograph Series, v. 179, p. 151-166.

Eberhart-Philips, D., D.H. Christensen, T.M. Brocher, R. Hasen, N.A. Ruppert, P.J. Haeussler, and G.A. Abers, 2006, Imaging the transition from Aleutian subduction to Yakutat collision in central Alaska, with local earthquakes and active source data: Journal of Geophysical Research Solid Earth, v. 111/B11303, 31 p.

Enkelmann, E., P.K. Zeitler, J.I. Garver, T.L. Pavlis, and B.P. Hooks, 2010, The thermochronological record of tectonic and surface process interaction at the Yukatat-North American collision zone in southeast Alaska: American Journal of Science, v. 310, p. 231-260.

Fuis, G.S., T.E. Moore, G. Plafker, T.M. Brocher, M.A. Fisher, W.D. Mooney, W.J. Nobleberg, R.A. Page, B.C. Beaudoin, N.I. Christensen, A.R. Levander, W.J. Lutter, R.W. Saltus, and N.A. Ruppert, 2008, Trans-Alaska crutal transect and continental evolution involving subduction underplating and synchronous foreland thrusting: Geology, v. 36, p. 267-270.

Hacker, B.R., P.B. Kelemen, M. Rioux, M.O. McWilliams, P.B. Glans, P.W. Reiners, P.W. Layer, U. Soderlund, and J.D. Vervoort, 2011, Thermochronology of the Talkeetna introceanic arc of Alaska; Ar/Ar, U-Th/He, Sm/Nd, and Lu/Hf dating: Tectonics, v. 301/, p. Citation TC1011.

Haeussler, P.J., R.L. Bruhn, and T.L. Pratt, 2000, Potential seismic hazards and tectonics of upper Cook Inlet basin, Alaska, based on analysis of Pliocene and younger deformation: GSA Bulletin, v. 112, p. 1414-1429.

Hoffman, M.D., and P.A. Armstrong, 2006, Miocene exhumation of the southern Talkeetna Mountains, south central Alaska, based on apatite (U-Th)/He thermochronology: GSA Abstracts with Programs, v. 38, p. 9.

Kveton, K.J., 1989, Structure, thermochronology, provenance, and tectonic history of the Orca Group in southwestern Prince William Sound, Alaska: Ph.D. Dissertation, University of Washington, 201 p.

Little, T.A., and C.W. Naeser, 1989, Tertiary tectonics of the Border Ranges fault systems, Chugach Mountains, Alaska – deformation and uplift in a fore-arc setting: *Journal of Geophysical Research Earth Planet*, v. 94, p. 4333-4359.

Parry, W.T., M.P. Bunds, R.L. Bruhn, C.M. Hall, and J.M. Murphy, 2001, Mineralogy, $^{40}\text{Ar}/^{39}\text{Ar}$ dating and apatite fission track track dating of rocks along the Castle Mountain fault, Alaska: *Tectonophysics*, v. 337, p. 149-172.

Willett, S.D., R. Slingerland, and N. Hovius, 2001, Uplift, shortening, and steady state topography in active mountain belts, *in* F.J. Pazzaglia, and P.L.K. Knuepfer, (eds.), *The steady-state orogeny, concepts, field observations, and models*: *American Journal of Science*, v. 301/4-5, p. 455-485.

Underplating below the western Chugach Mountains in the southern Alaska block syntaxial core constrained by low-temperature thermochronology

Sean M. Hartman*★

Phillip A. Armstrong*

Jenny Arkle*

Peter Haeussler♦

*California State University, Fullerton

★University of Southern California

♦USGS Alaska

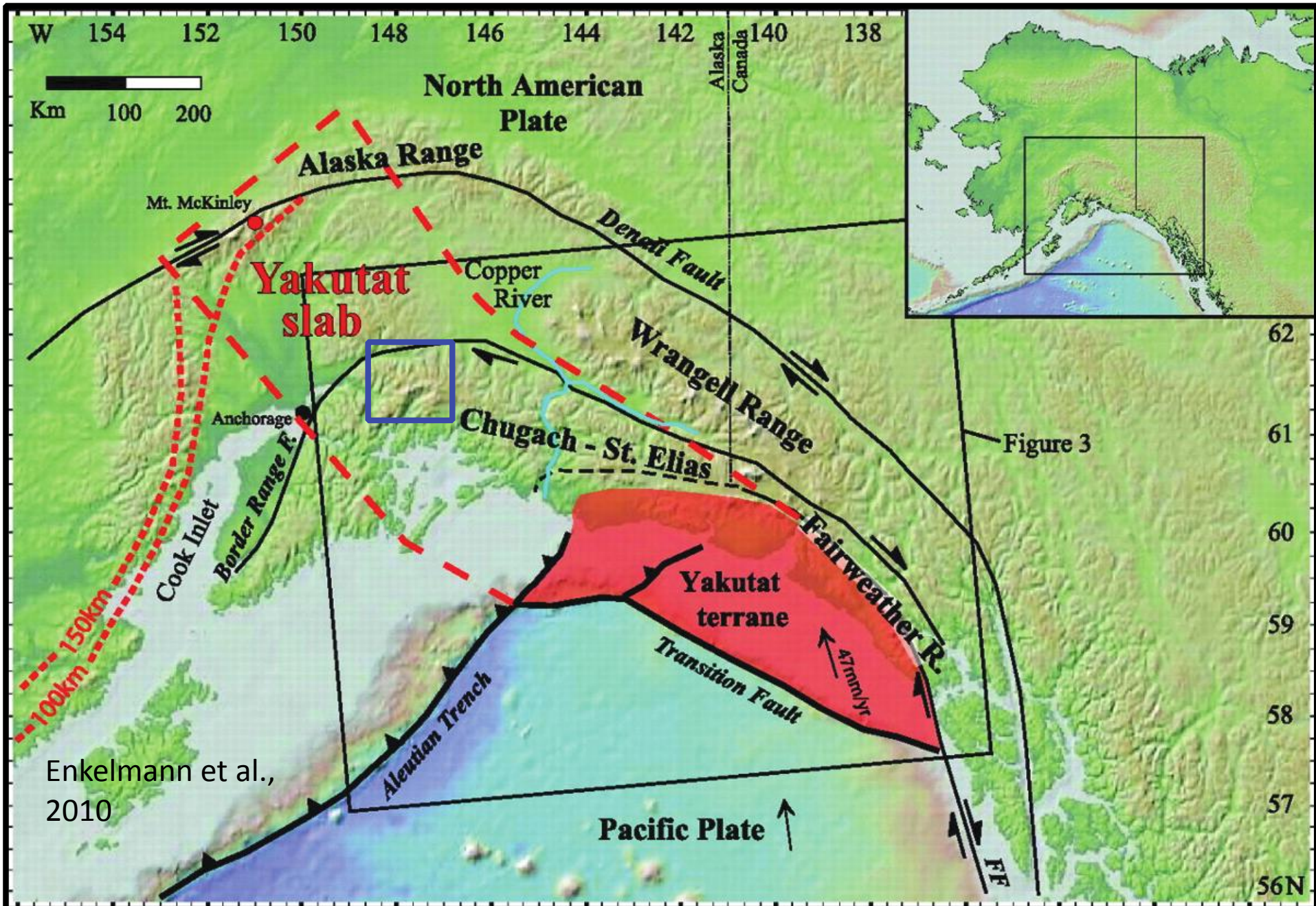


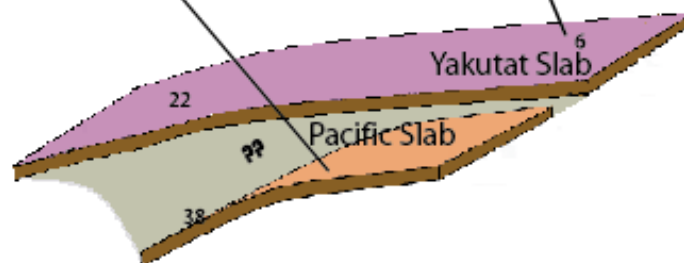
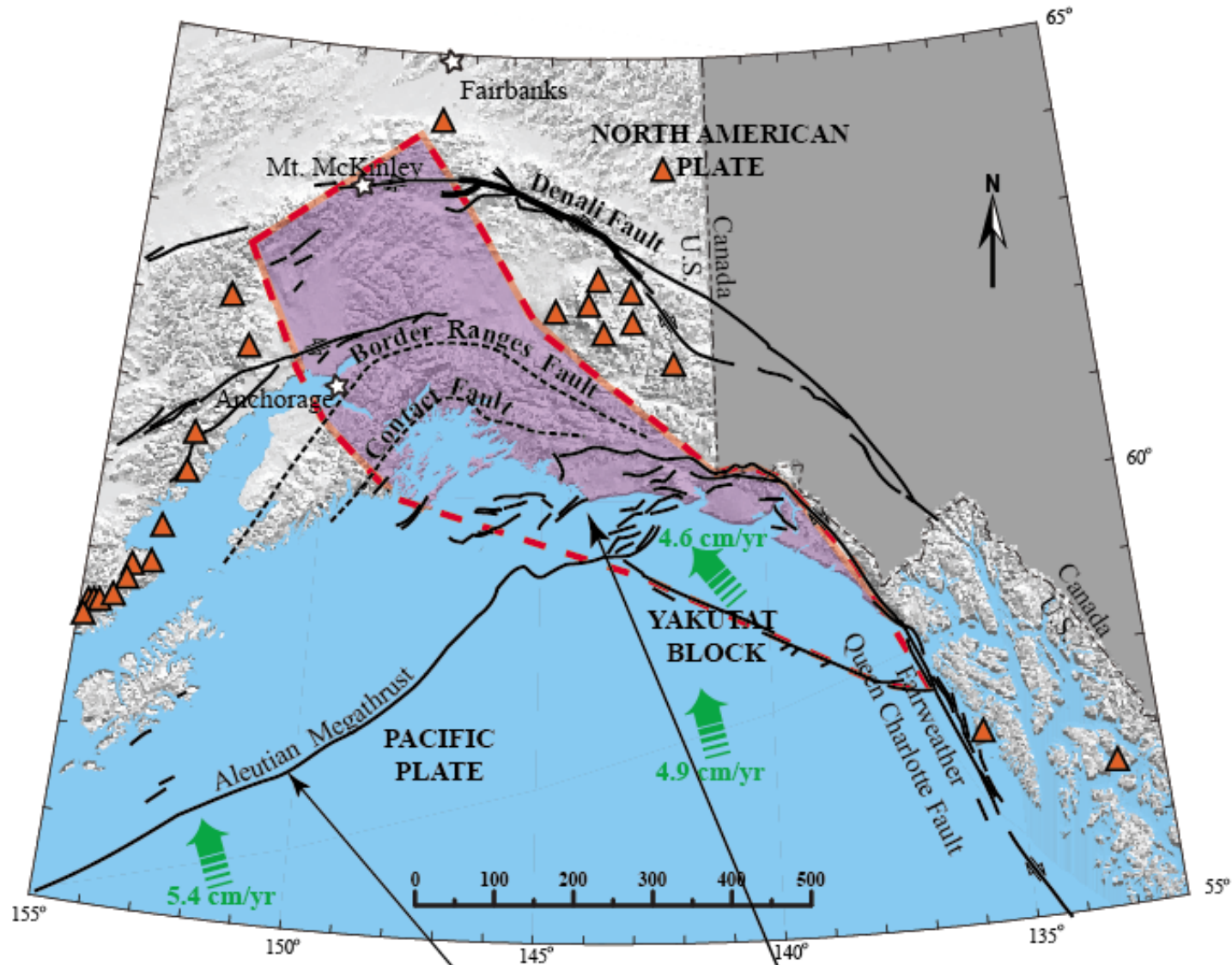
Presenter's notes: Today I want to talk about my research addressing the spatial and temporal patterns of rock uplift and exhumation in the syntaxial core of the western Chugach Mountains of southern Alaska constrained by the apatite helium low temperature thermochronometer

Outline

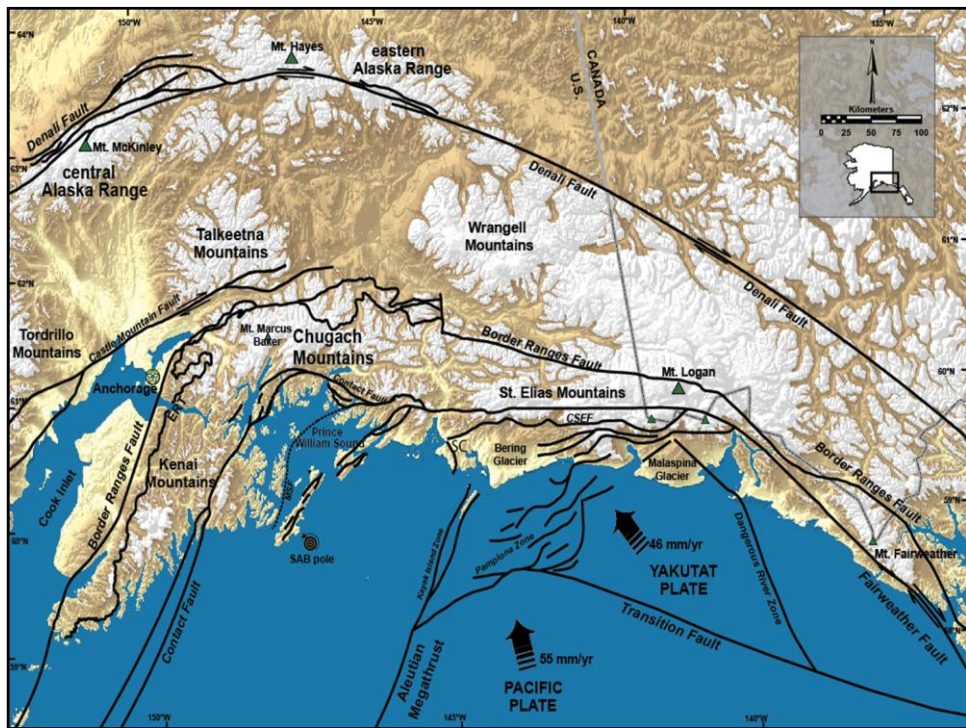
- Geological background
- Problem to be addressed
- Hypothesis
- Testing
- Results
- Interpretation
- Summary

Geologic Background





**Haeussler et al.
(2000) and Eberhart-
Phillips et al. (2006)**

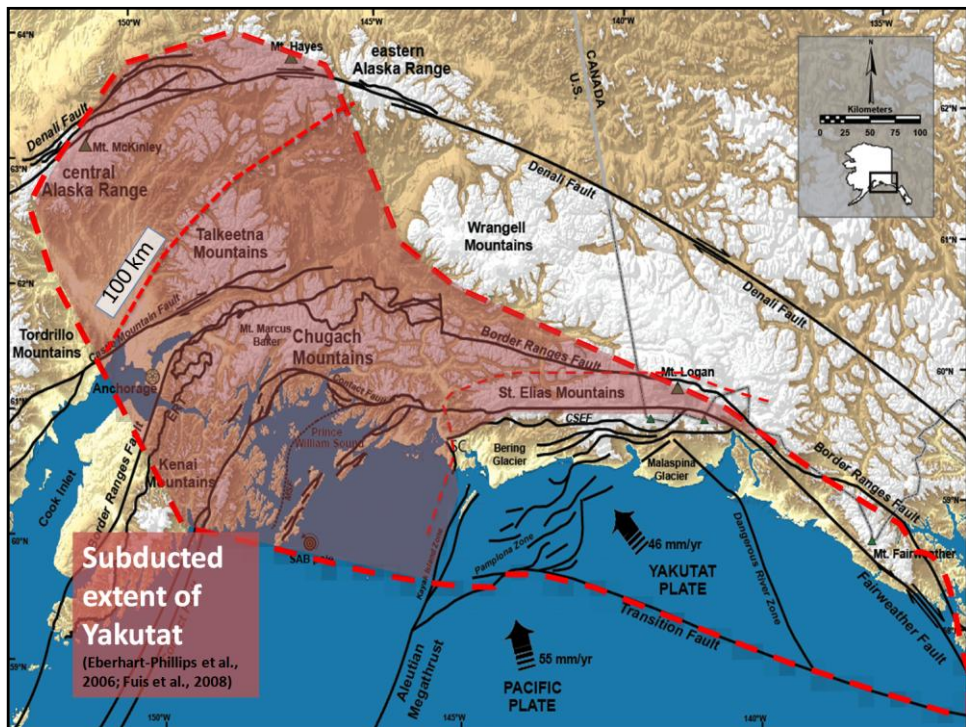


Presenter's notes: Map showing major topography and faults

Main point here is that major fault systems and topographic grain make CCW bends from SE to NW

Major bends in DF at Mt Hayes area and Denali

Major bends in BRF, CSEF systems



Presenter's notes: Lateral extent based on Eberhart Phillips and Fuis (2008) – loosely constrained

Megathrust dips 6 deg

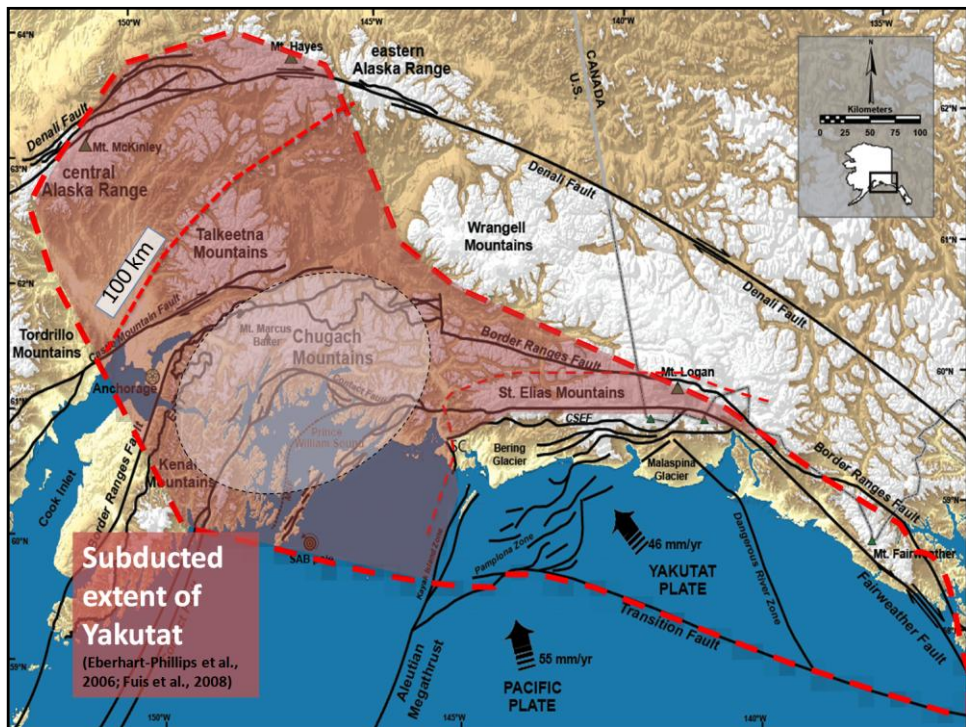
Steepens to north – show 100 km

Inboard area – but effects of Yakutat extend farther north and east

Outboard region – northward extent of the Aleutian megathrust

In between region – fault and topographic systems have maximum curvature and bend to south. 20-25 km above megathrust

NEXT SLIDE WILL BE IN BOARD REGION – NOTE LOCATION ON MAP



Presenter's notes: Lateral extent based on Eberhart Phillips and Fuis (2008) – loosely constrained

Megathrust dips 6 deg

Steepens to north – show 100 km

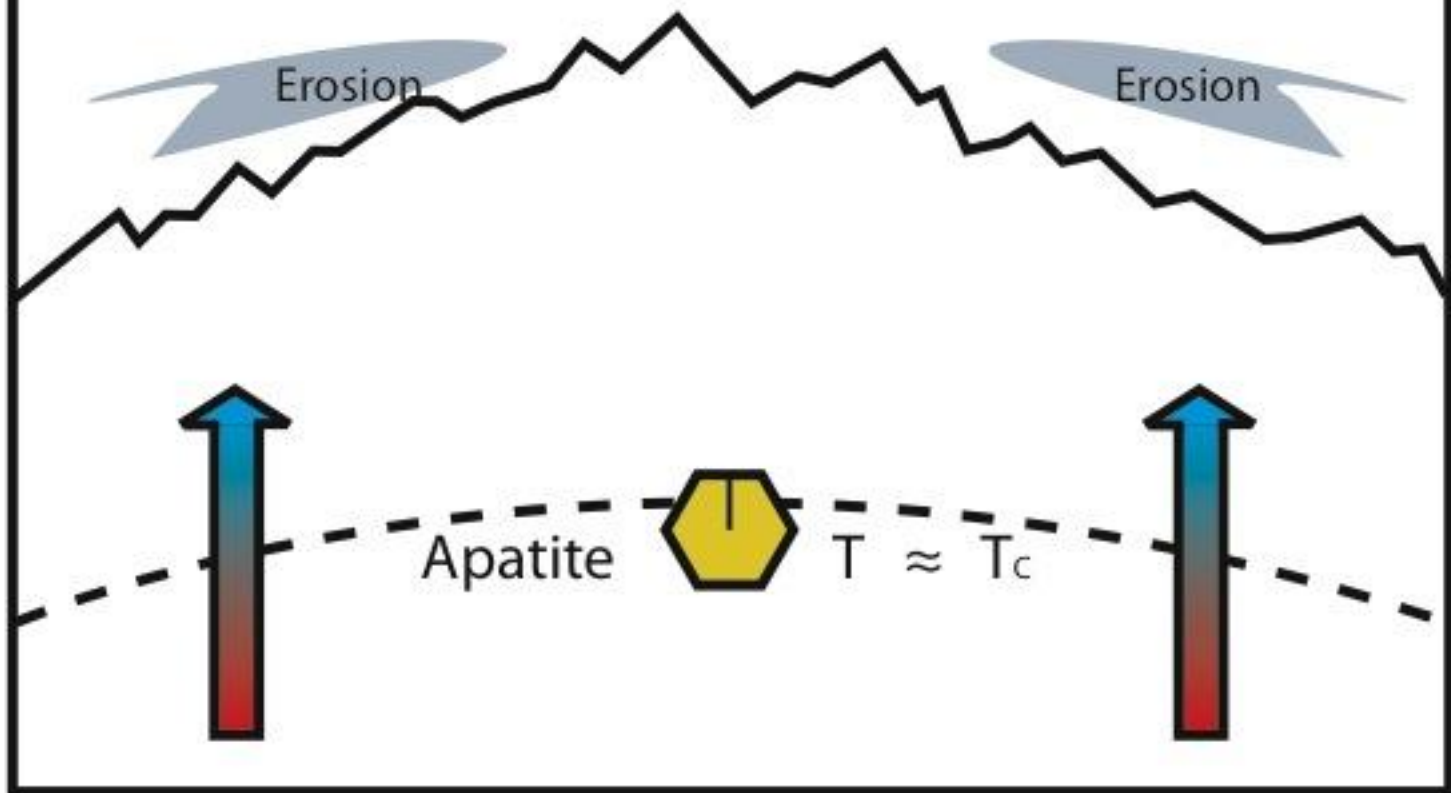
Inboard area – but effects of Yakutat extend farther north and east

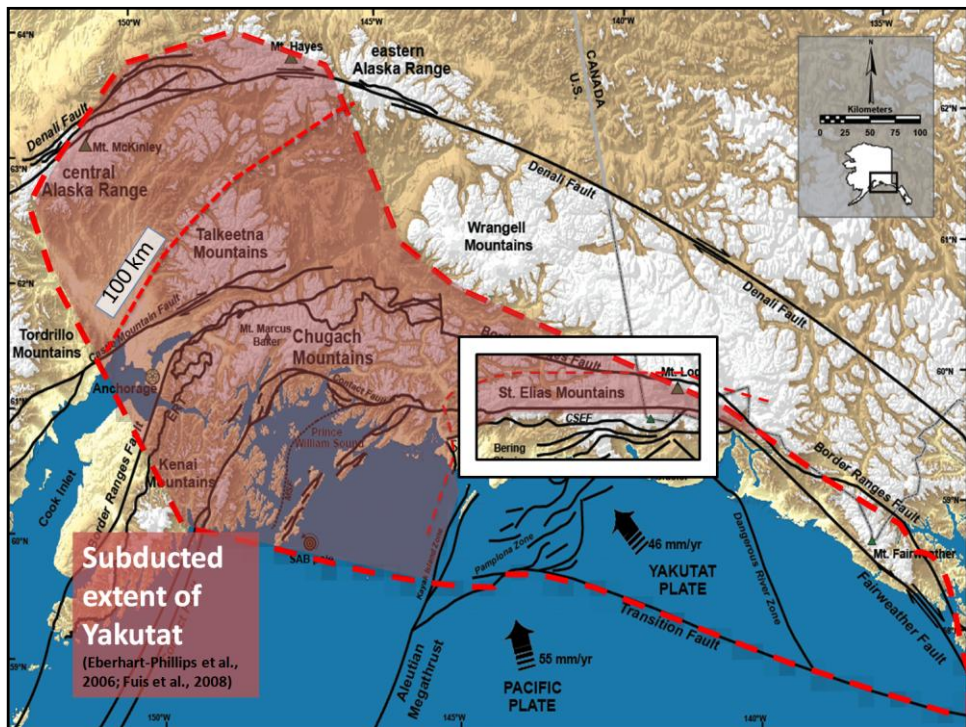
Outboard region – northward extent of the Aleutian megathrust

In between region – fault and topographic systems have maximum curvature and bend to south. 20-25 km above megathrust

NEXT SLIDE WILL BE IN BOARD REGION – NOTE LOCATION ON MAP

Partial diffusion/retention of ^4He ($\sim 60^\circ$)





Presenter's notes: Lateral extent based on Eberhart Phillips and Fuis (2008) – loosely constrained

Megathrust dips 6 deg

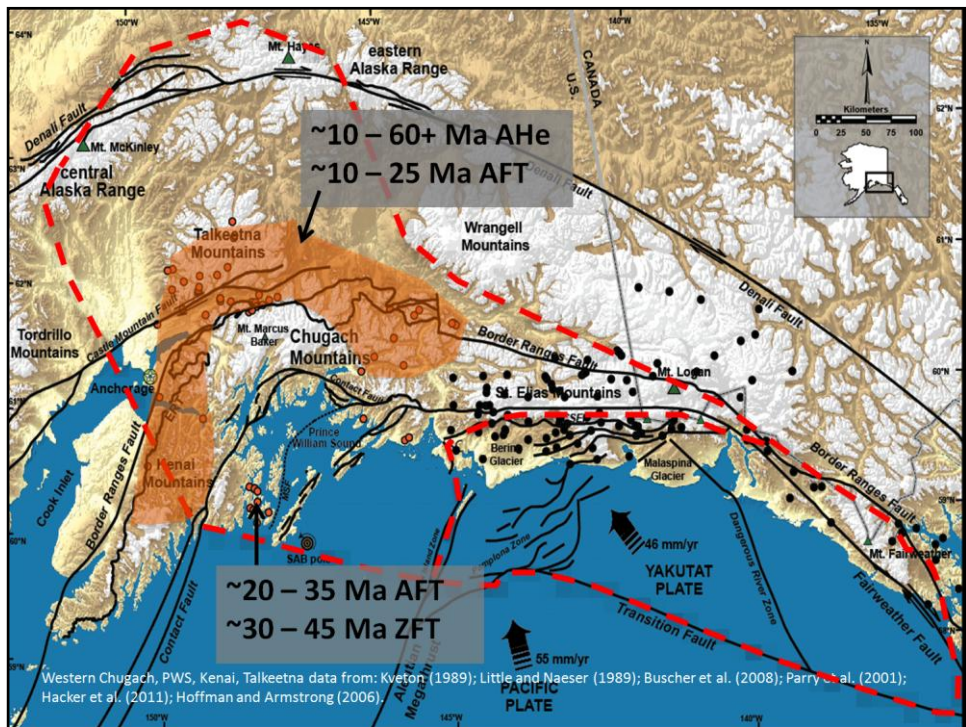
Steepens to north – show 100 km

Inboard area – but effects of Yakutat extend farther north and east

Outboard region – northward extent of the Aleutian megathrust

In between region – fault and topographic systems have maximum curvature and bend to south. 20-25 km above megathrust

NEXT SLIDE WILL BE IN BOARD REGION – NOTE LOCATION ON MAP



Presenter's notes: Area centered above Yakutat

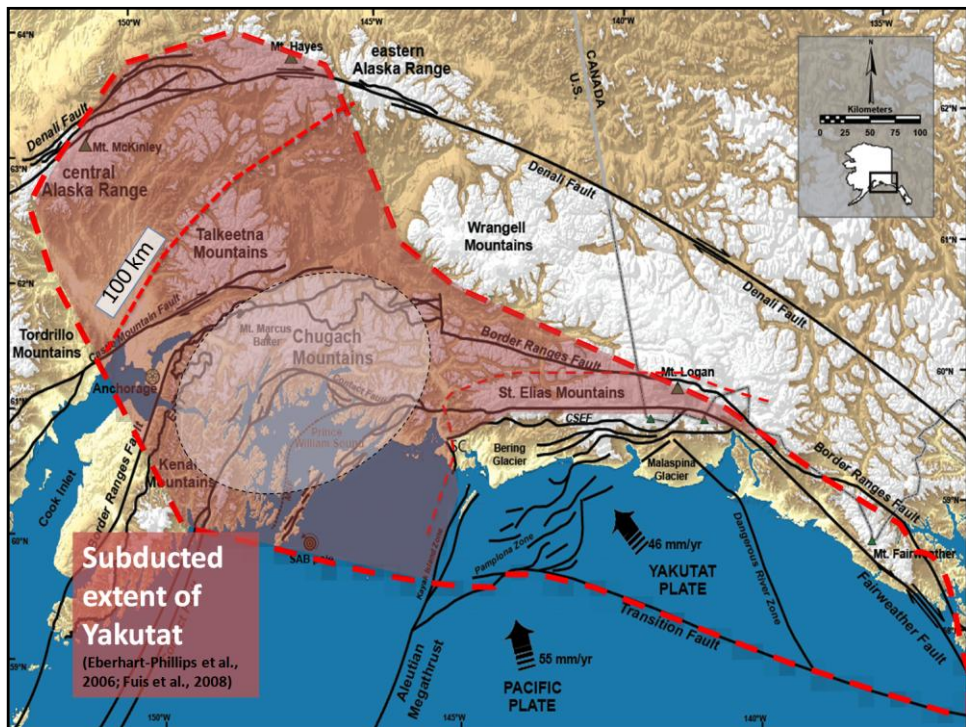
Maximum curvature

Contact fault

Several thermochron studies over last couple decades, but all around the periphery of PWS – CM core as outlined by faults and topography

Ages – AFT 10 – 25 and AHe 10-60 Ma in the bow wave around the what we call 'syntaxial' core.

Farther south, Kveton has AFT of 20-35 and ZFT of 30-45



Presenter's notes: Lateral extent based on Eberhart Phillips and Fuis (2008) – loosely constrained

Megathrust dips 6 deg

Steepens to north – show 100 km

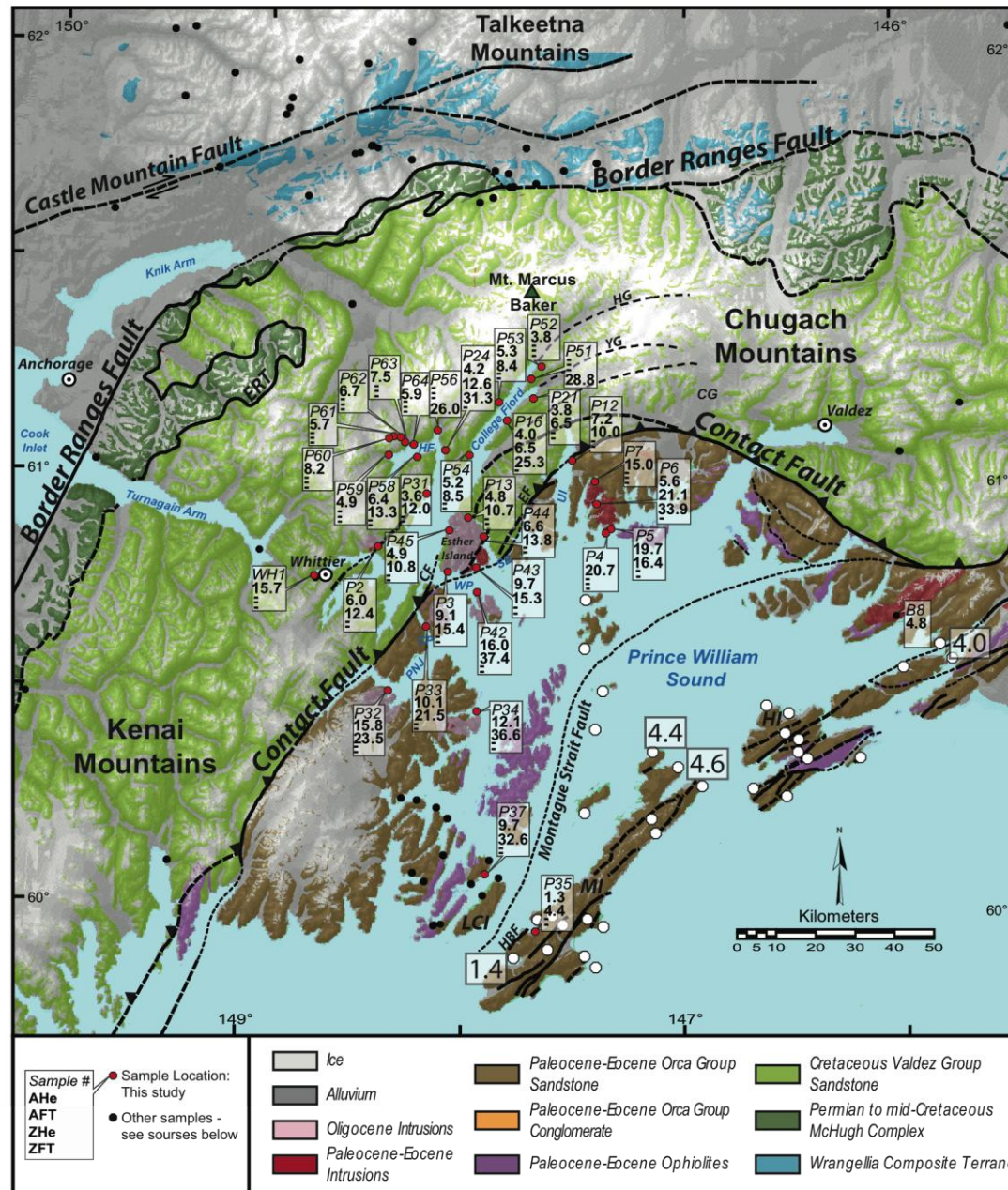
Inboard area – but effects of Yakutat extend farther north and east

Outboard region – northward extent of the Aleutian megathrust

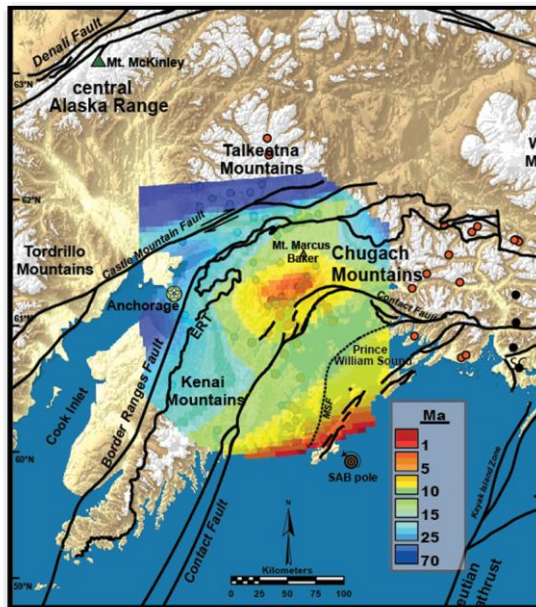
In between region – fault and topographic systems have maximum curvature and bend to south. 20-25 km above megathrust

NEXT SLIDE WILL BE IN BOARD REGION – NOTE LOCATION ON MAP

Problem to be Addressed



Hypothesis



Apatite He ages

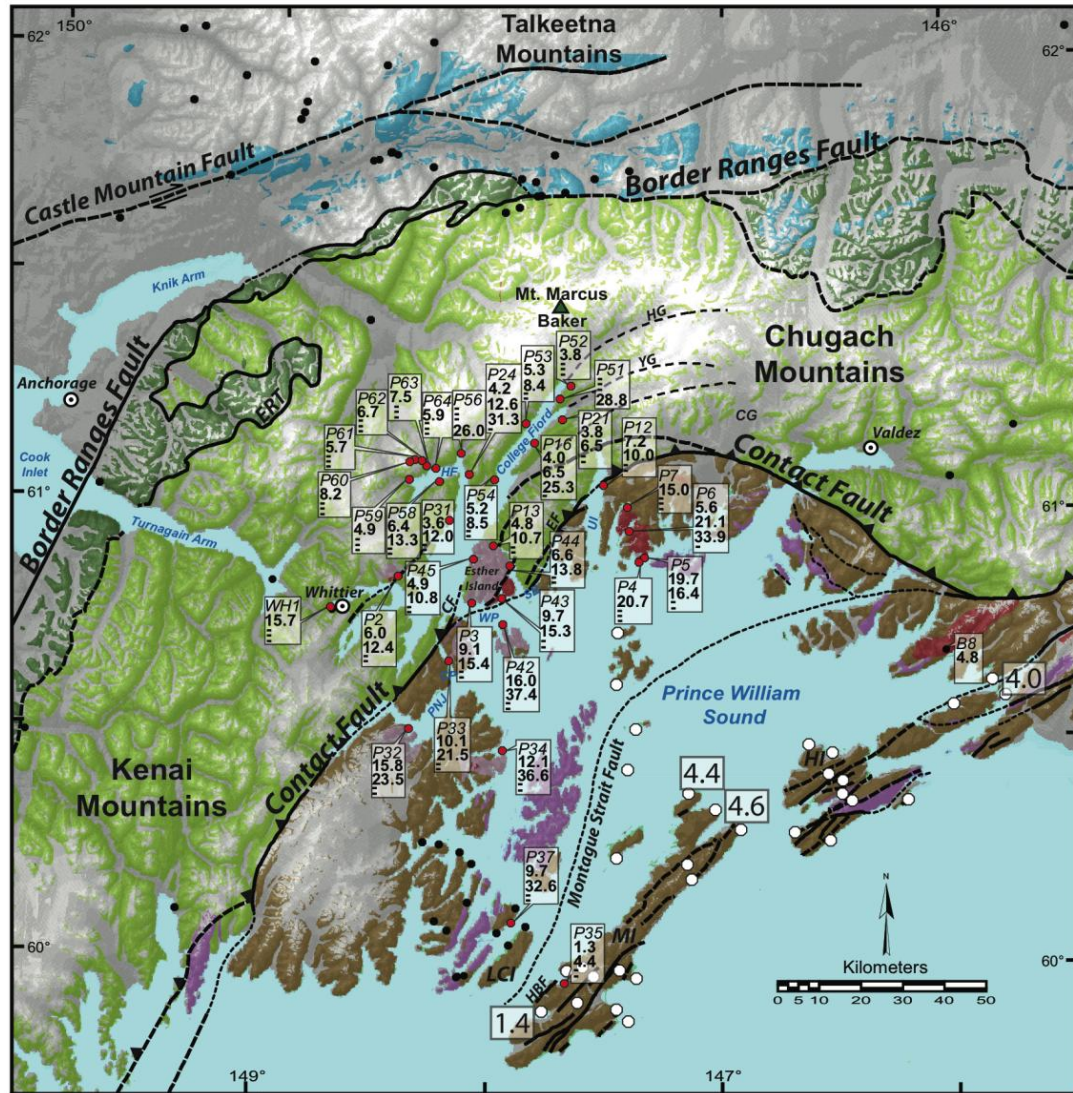
3-4 Ma in core

Increase
radially
outward.

Presenter's notes: Ahe ages decrease into core of CM. But youngest ages (3-4 Ma) are concentrated on the south side of range and adjacent to CF – will be important in later plots
AFT ages show same trends

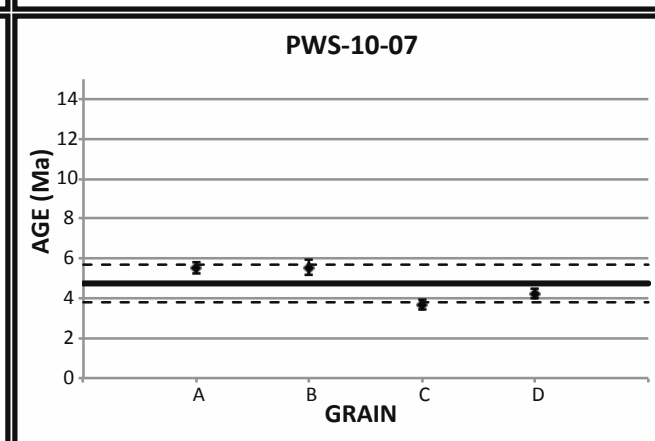
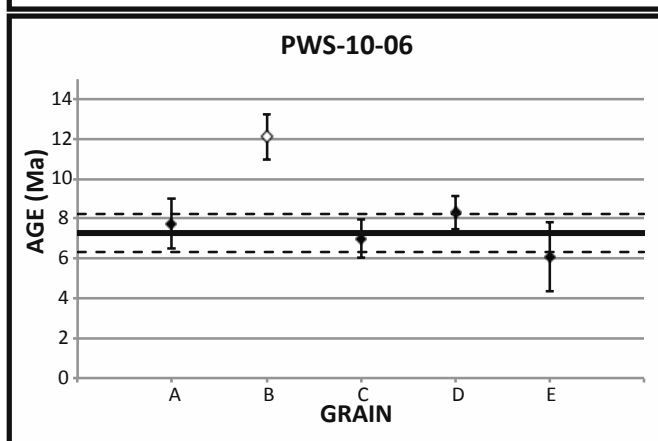
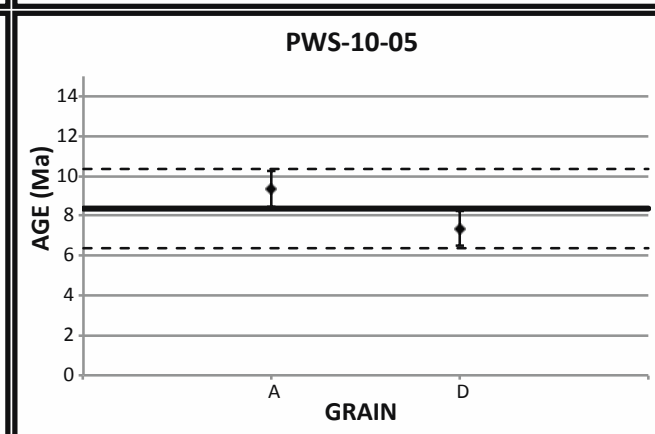
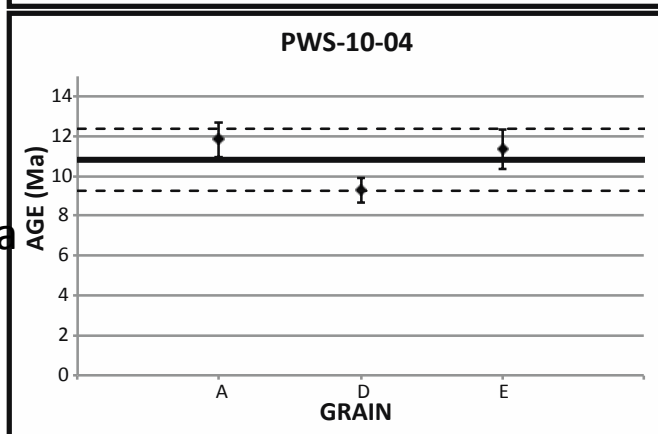
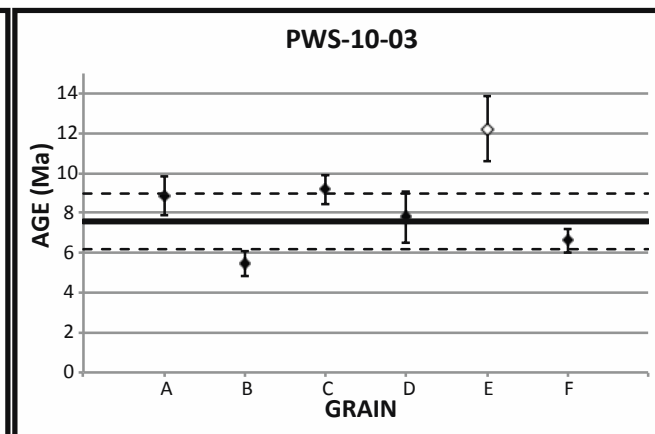
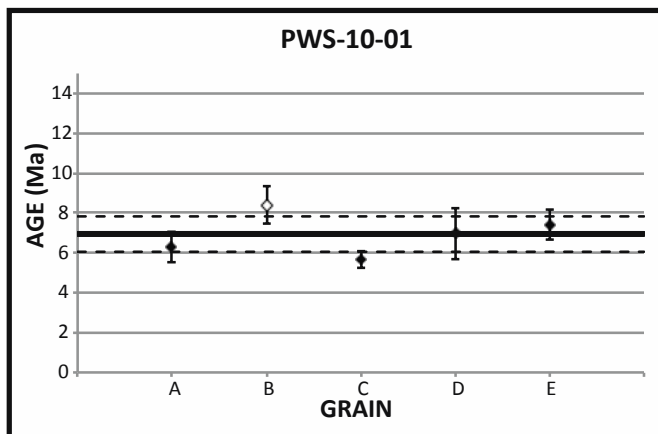
Testing

This figure is a detailed geological map of the Chugach Mountains area in Alaska, centered around the Whittier and Anchorage regions. The map displays various geological units, faults, and sample locations. Key features include the Kenai Mountains to the west, the Chugach Mountains to the east, and the Prince William Sound to the south. Major faults shown are the Castle Mountain Fault, Border Ranges Fault, Contact Fault, and Montague Strait Fault. Sample locations are marked with red dots and labeled with sample numbers (e.g., P1, P2, P3, P4, P5, P6, P7, P8, P9, P10, P11, P12, P13, P14, P15, P16, P17, P18, P19, P20, P21, P22, P23, P24, P25, P26, P27, P28, P29, P30, P31, P32, P33, P34, P35, P36, P37, P38, P39, P40, P41, P42, P43, P44, P45, P46, P47, P48, P49, P50, P51, P52, P53, P54, P55, P56, P57, P58, P59, P60, P61, P62, P63, P64, P65, P66, P67, P68, P69, P70, P71, P72, P73, P74, P75, P76, P77, P78, P79, P80, P81, P82, P83, P84, P85, P86, P87, P88, P89, P90, P91, P92, P93, P94, P95, P96, P97, P98, P99, P100, P101, P102, P103, P104, P105, P106, P107, P108, P109, P110, P111, P112, P113, P114, P115, P116, P117, P118, P119, P120, P121, P122, P123, P124, P125, P126, P127, P128, P129, P130, P131, P132, P133, P134, P135, P136, P137, P138, P139, P140, P141, P142, P143, P144, P145, P146, P147, P148, P149, P150, P151, P152, P153, P154, P155, P156, P157, P158, P159, P160, P161, P162, P163, P164, P165, P166, P167, P168, P169, P170, P171, P172, P173, P174, P175, P176, P177, P178, P179, P180, P181, P182, P183, P184, P185, P186, P187, P188, P189, P190, P191, P192, P193, P194, P195, P196, P197, P198, P199, P200, P201, P202, P203, P204, P205, P206, P207, P208, P209, P210, P211, P212, P213, P214, P215, P216, P217, P218, P219, P220, P221, P222, P223, P224, P225, P226, P227, P228, P229, P230, P231, P232, P233, P234, P235, P236, P237, P238, P239, P240, P241, P242, P243, P244, P245, P246, P247, P248, P249, P250, P251, P252, P253, P254, P255, P256, P257, P258, P259, P260, P261, P262, P263, P264, P265, P266, P267, P268, P269, P270, P271, P272, P273, P274, P275, P276, P277, P278, P279, P280, P281, P282, P283, P284, P285, P286, P287, P288, P289, P290, P291, P292, P293, P294, P295, P296, P297, P298, P299, P300, P301, P302, P303, P304, P305, P306, P307, P308, P309, P310, P311, P312, P313, P314, P315, P316, P317, P318, P319, P320, P321, P322, P323, P324, P325, P326, P327, P328, P329, P330, P331, P332, P333, P334, P335, P336, P337, P338, P339, P340, P341, P342, P343, P344, P345, P346, P347, P348, P349, P350, P351, P352, P353, P354, P355, P356, P357, P358, P359, P360, P361, P362, P363, P364, P365, P366, P367, P368, P369, P370, P371, P372, P373, P374, P375, P376, P377, P378, P379, P380, P381, P382, P383, P384, P385, P386, P387, P388, P389, P390, P391, P392, P393, P394, P395, P396, P397, P398, P399, P400, P401, P402, P403, P404, P405, P406, P407, P408, P409, P410, P411, P412, P413, P414, P415, P416, P417, P418, P419, P420, P421, P422, P423, P424, P425, P426, P427, P428, P429, P430, P431, P432, P433, P434, P435, P436, P437, P438, P439, P440, P441, P442, P443, P444, P445, P446, P447, P448, P449, P450, P451, P452, P453, P454, P455, P456, P457, P458, P459, P460, P461, P462, P463, P464, P465, P466, P467, P468, P469, P470, P471, P472, P473, P474, P475, P476, P477, P478, P479, P480, P481, P482, P483, P484, P485, P486, P487, P488, P489, P490, P491, P492, P493, P494, P495, P496, P497, P498, P499, P500, P501, P502, P503, P504, P505, P506, P507, P508, P509, P510, P511, P512, P513, P514, P515, P516, P517, P518, P519, P520, P521, P522, P523, P524, P525, P526, P527, P528, P529, P530, P531, P532, P533, P534, P535, P536, P537, P538, P539, P540, P541, P542, P543, P544, P545, P546, P547, P548, P549, P550, P551, P552, P553, P554, P555, P556, P557, P558, P559, P560, P561, P562, P563, P564, P565, P566, P567, P568, P569, P570, P571, P572, P573, P574, P575, P576, P577, P578, P579, P580, P581, P582, P583, P584, P585, P586, P587, P588, P589, P590, P591, P592, P593, P594, P595, P596, P597, P598, P599, P600, P601, P602, P603, P604, P605, P606, P607, P608, P609, P610, P611, P612, P613, P614, P615, P616, P617, P618, P619, P620, P621, P622, P623, P624, P625, P626, P627, P628, P629, P630, P631, P632, P633, P634, P635, P636, P637, P638, P639, P640, P641, P642, P643, P644, P645, P646, P647, P648, P649, P650, P651, P652, P653, P654, P655, P656, P657, P658, P659, P660, P661, P662, P663, P664, P665, P666, P667, P668, P669, P670, P671, P672, P673, P674, P675, P676, P677, P678, P679, P680, P681, P682, P683, P684, P685, P686, P687, P688, P689, P690, P691, P692, P693, P694, P695, P696, P697, P698, P699, P700, P701, P702, P703, P704, P705, P706, P707, P708, P709, P710, P711, P712, P713, P714, P715, P716, P717, P718, P719, P720, P721, P722, P723, P724, P725, P726, P727, P728, P729, P730, P731, P732, P733, P734, P735, P736, P737, P738, P739, P740, P741, P742, P743, P744, P745, P746, P747, P748, P749, P750, P751, P752, P753, P754, P755, P756, P757, P758, P759, P760, P761, P762, P763, P764, P765, P766, P767, P768, P769, P770, P771, P772, P773, P774, P775, P776, P777, P778, P779, P780, P781, P782, P783, P784, P785, P786, P787, P788, P789, P790, P791, P792, P793, P794, P795, P796, P797, P798, P799, P800, P801, P802, P803, P804, P805, P806, P807, P808, P809, P810, P811, P812,









6.9 ± 0.9 Ma

7.6 ± 1.4 Ma

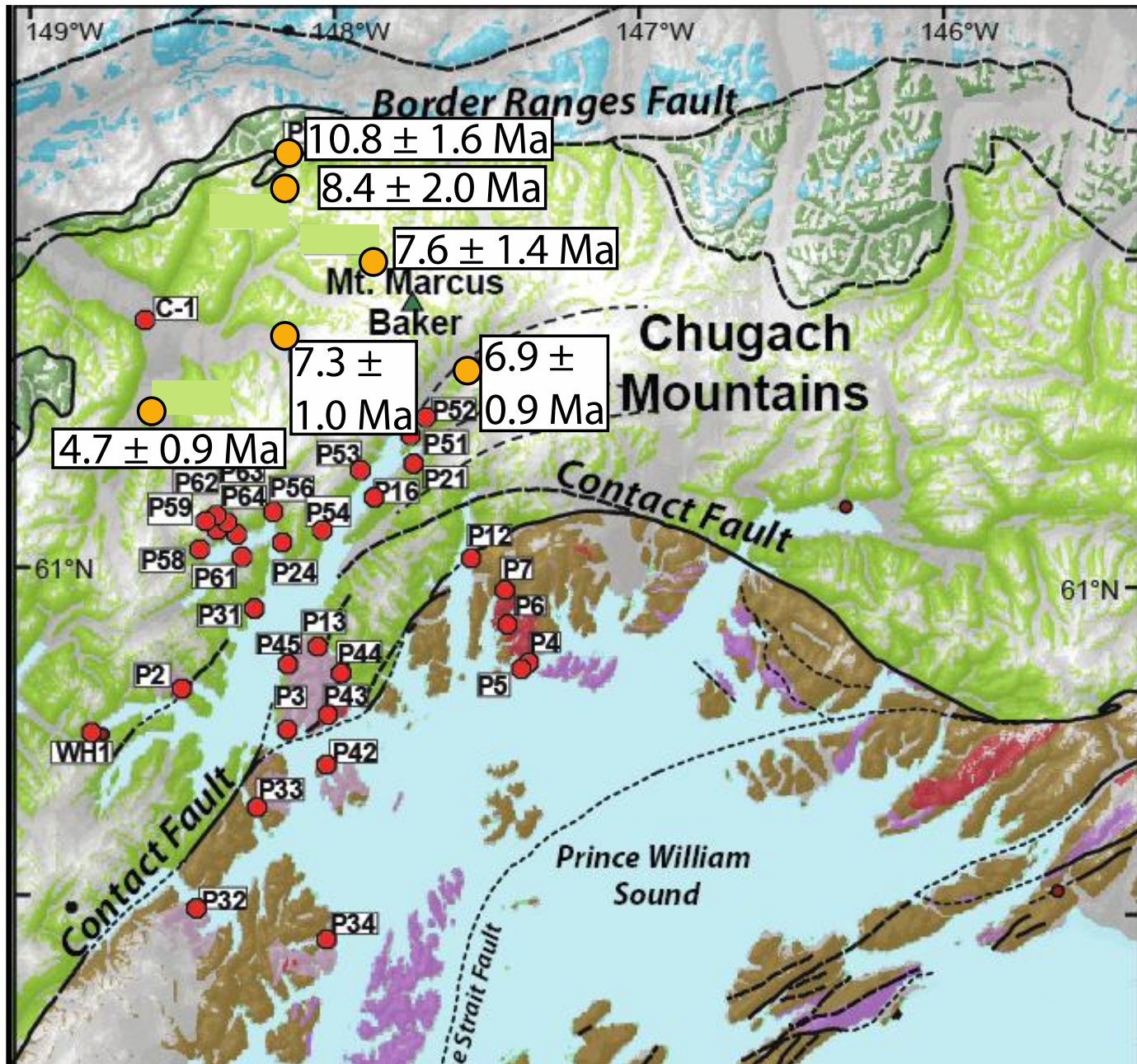
10.8 ± 1.6 Ma

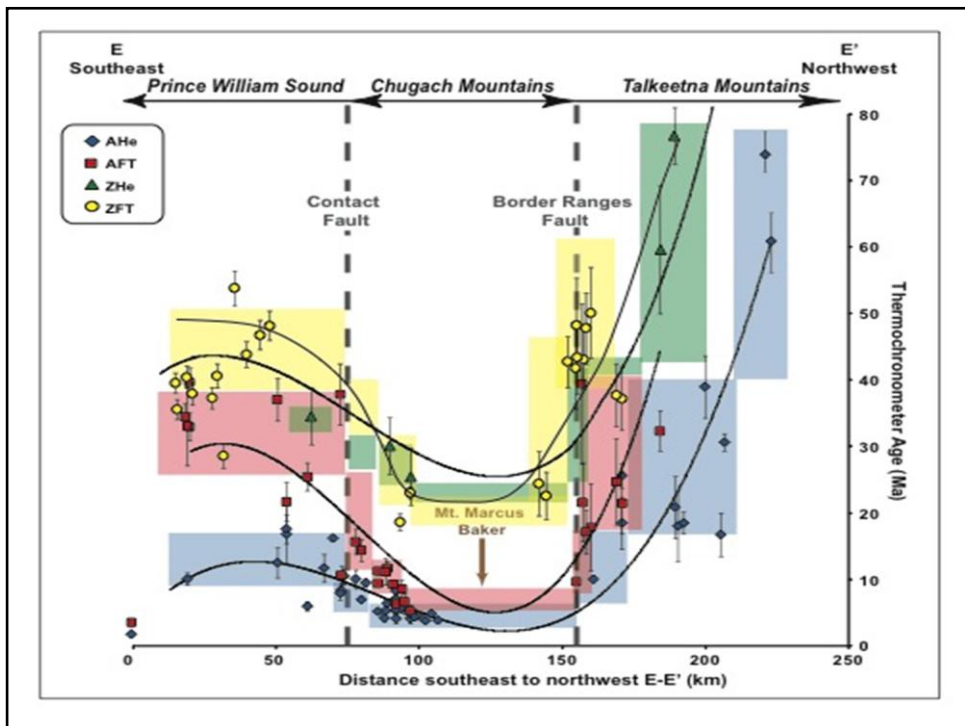
8.4 ± 2.0 Ma

7.3 ± 1.0 Ma

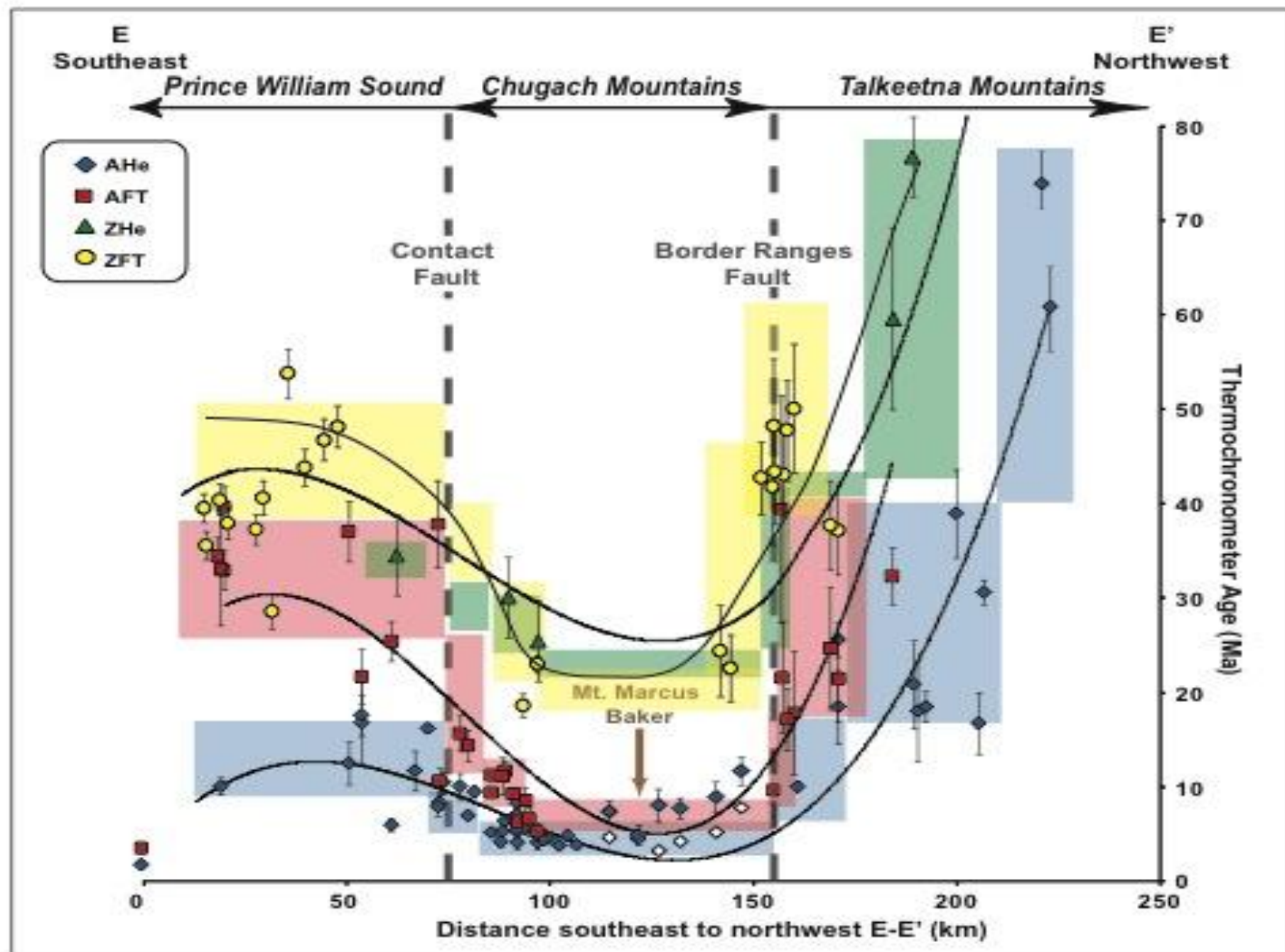
4.7 ± 0.9 Ma

Results

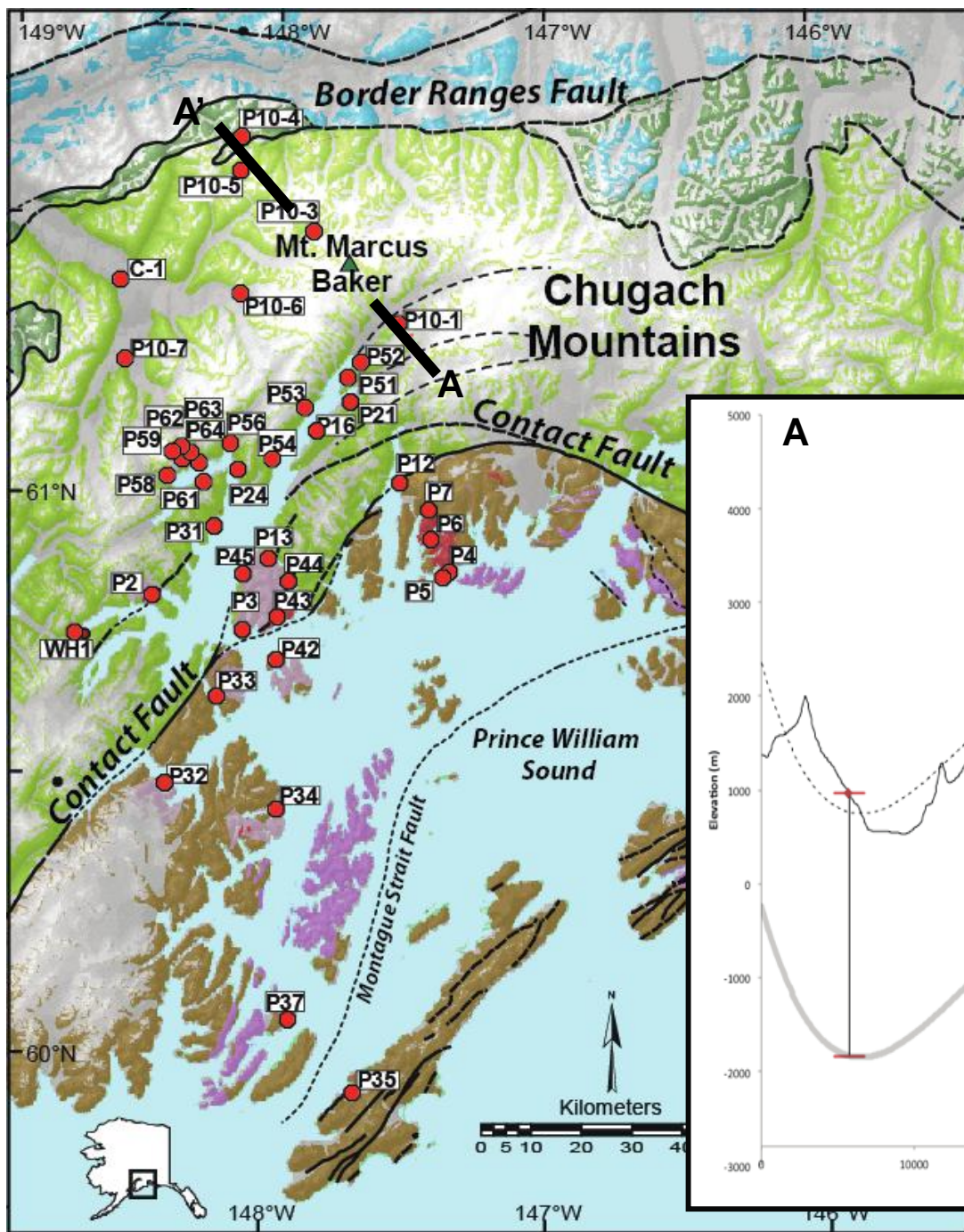




Presenter's notes: Ages sea level



$$\text{Rate of Exhumation} = \frac{Z_{Tc}}{\text{Mean Age}}$$

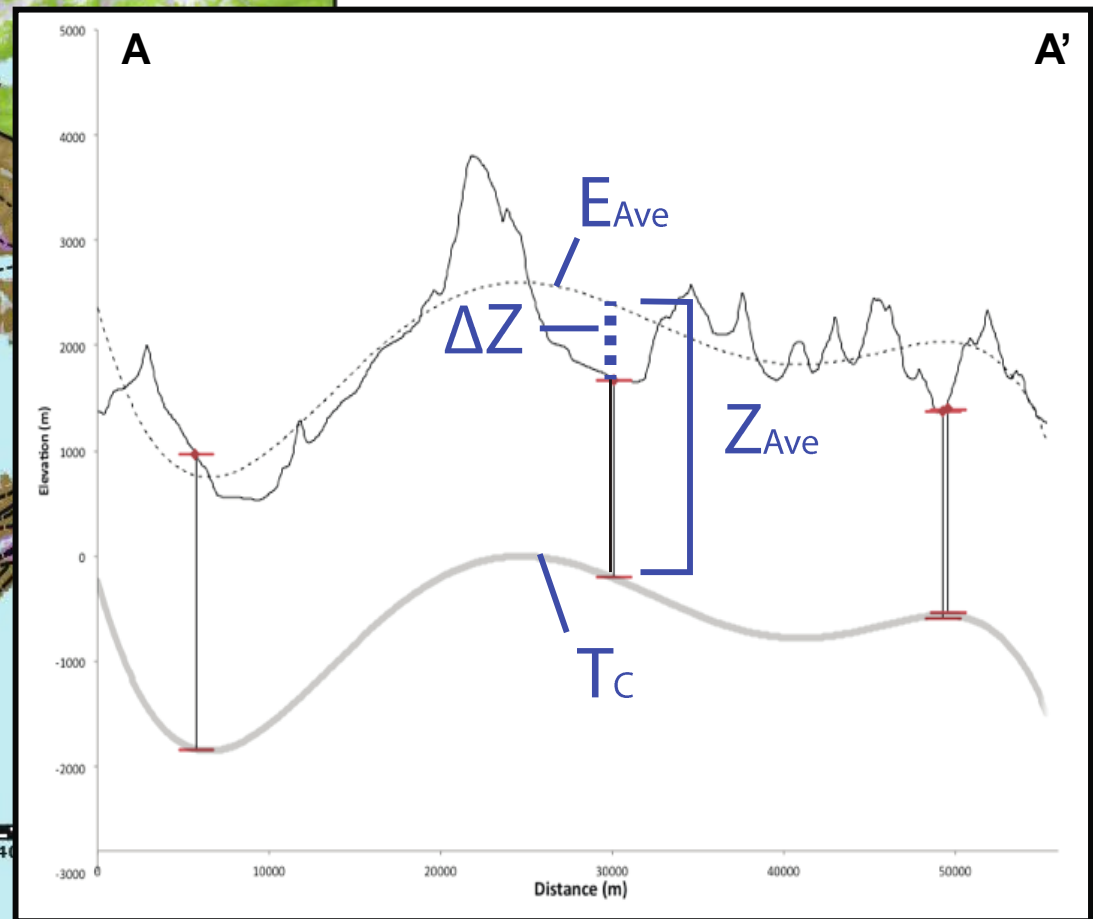


T_c = Closure T.

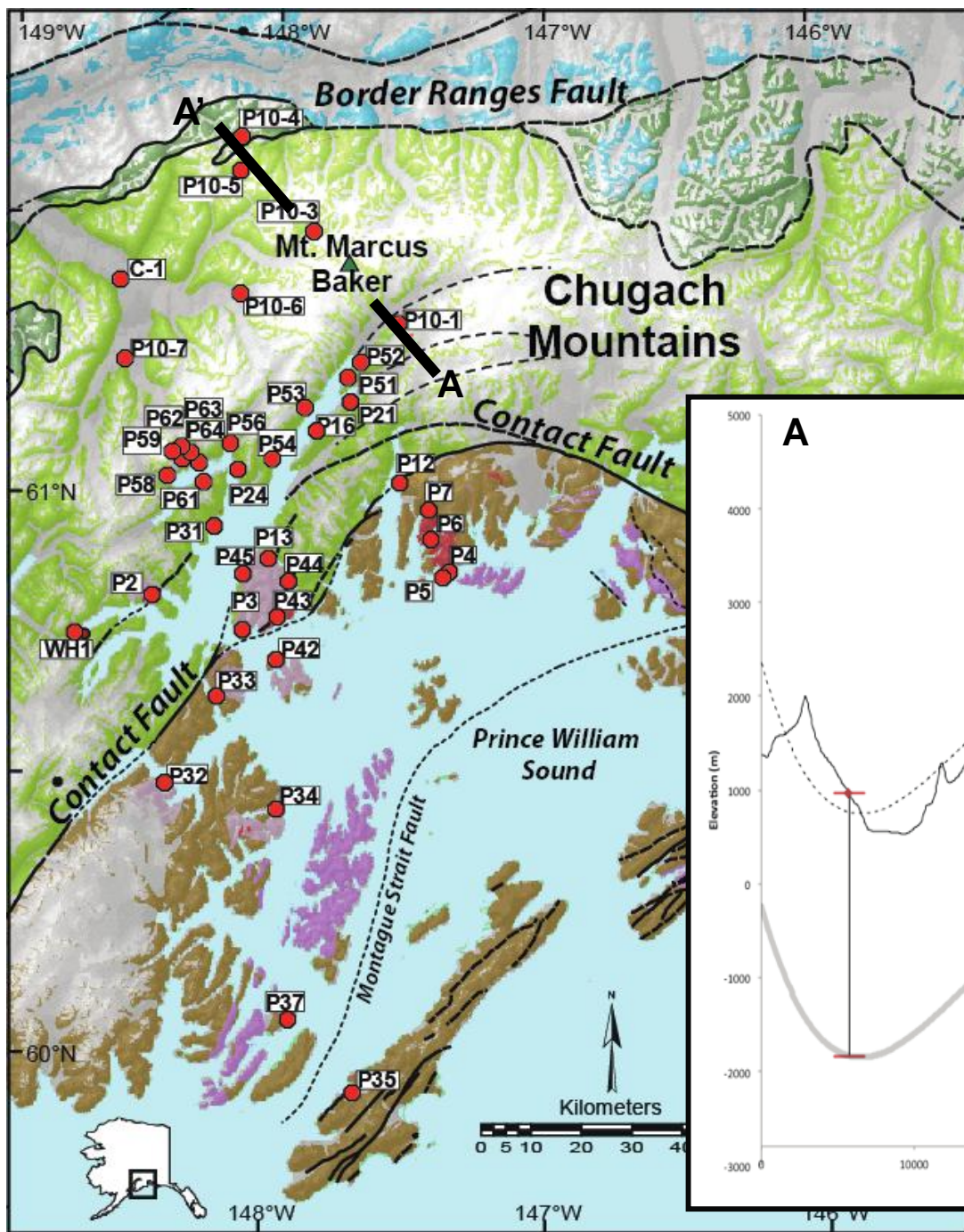
Z_{Ave} = Ave. Depth to T_c

E_{Ave} = Ave. Elevation

ΔZ = Difference Elev.







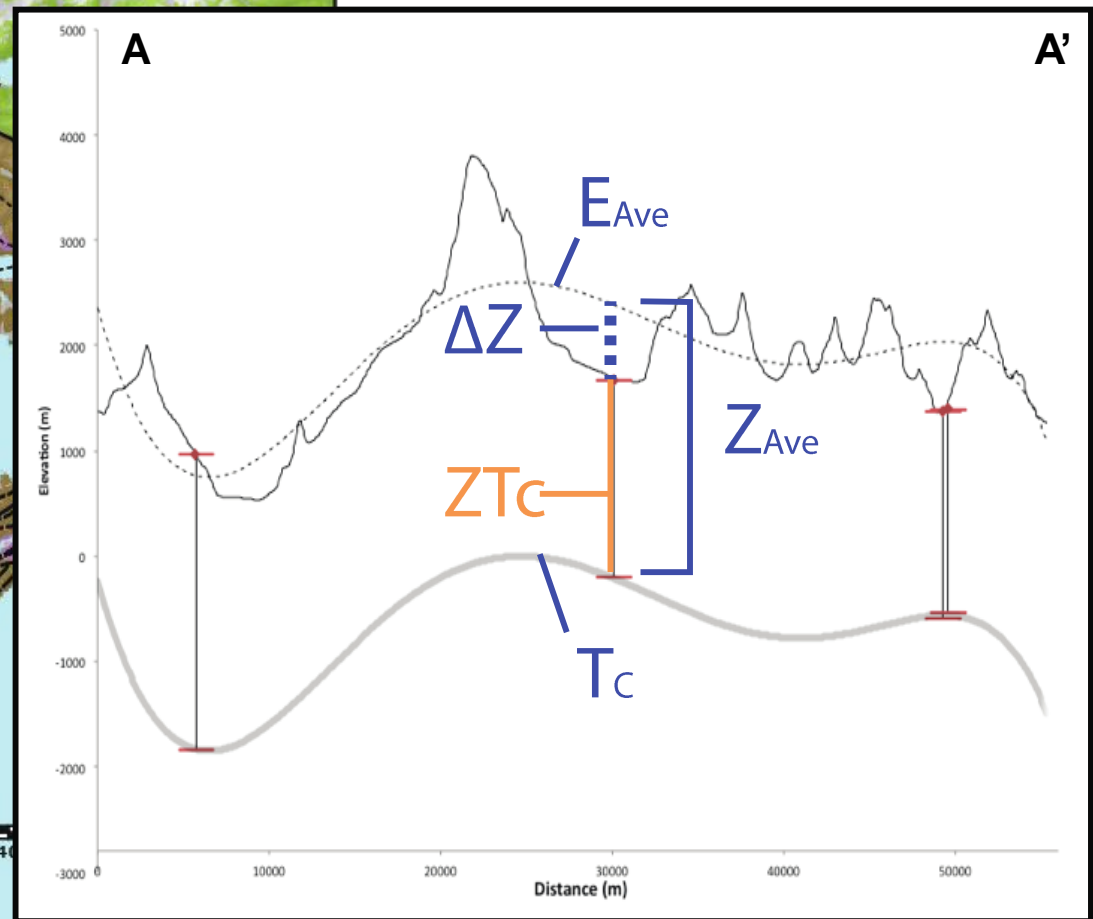
T_c = Closure T.

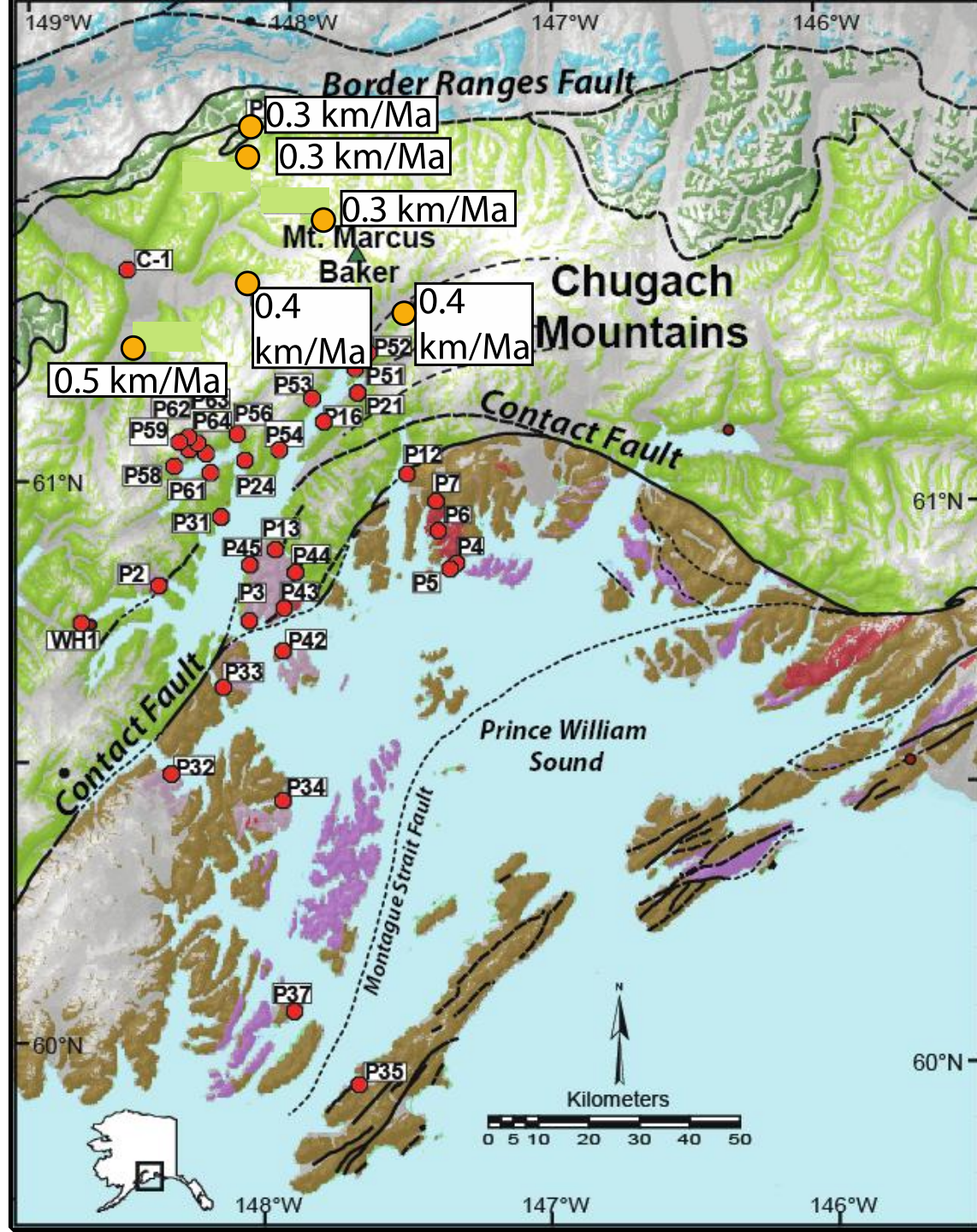
Z_{Ave} = Ave. Depth to T_c

E_{Ave} = Ave. Elevation

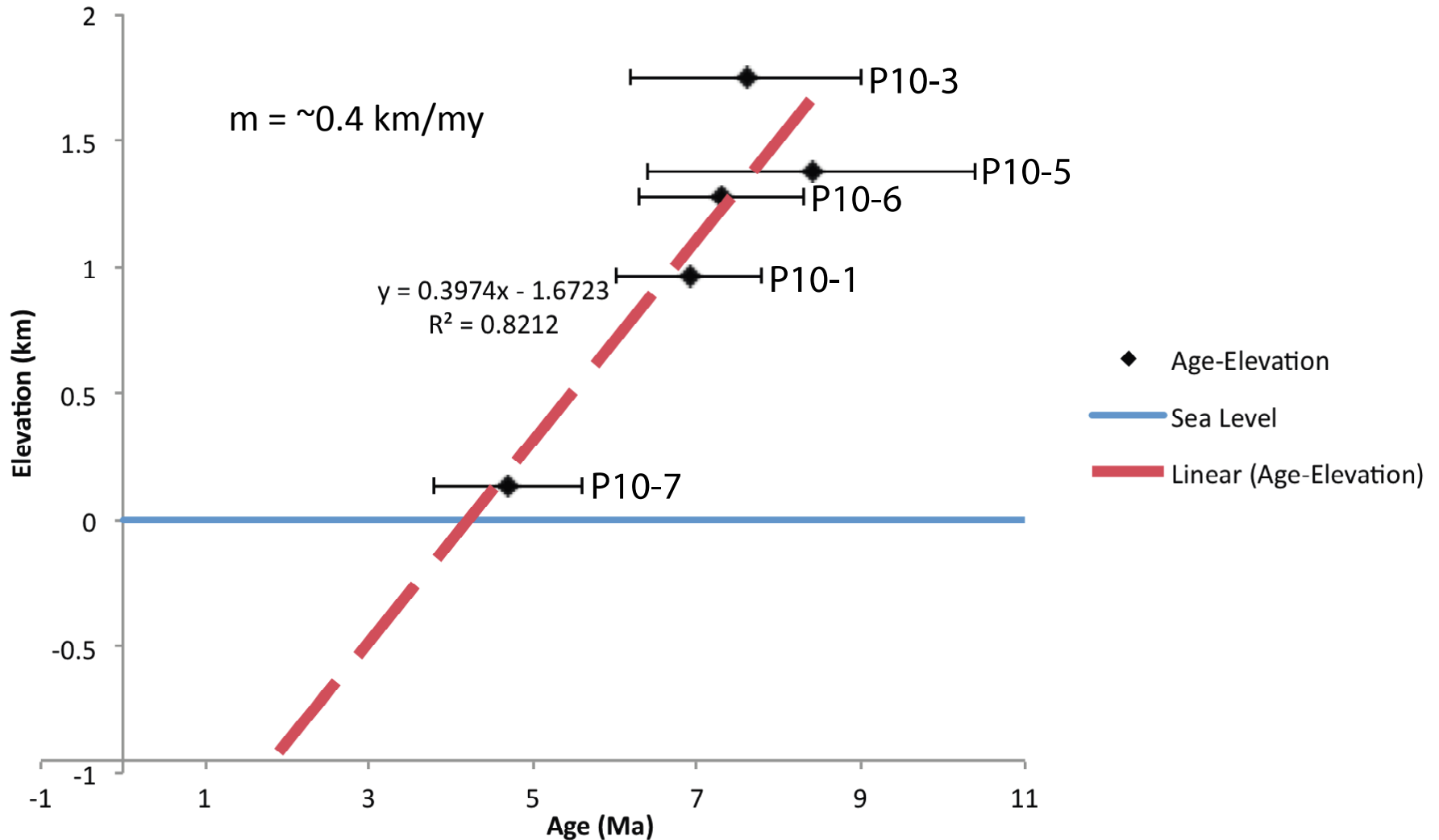
ΔZ = Difference Elev.

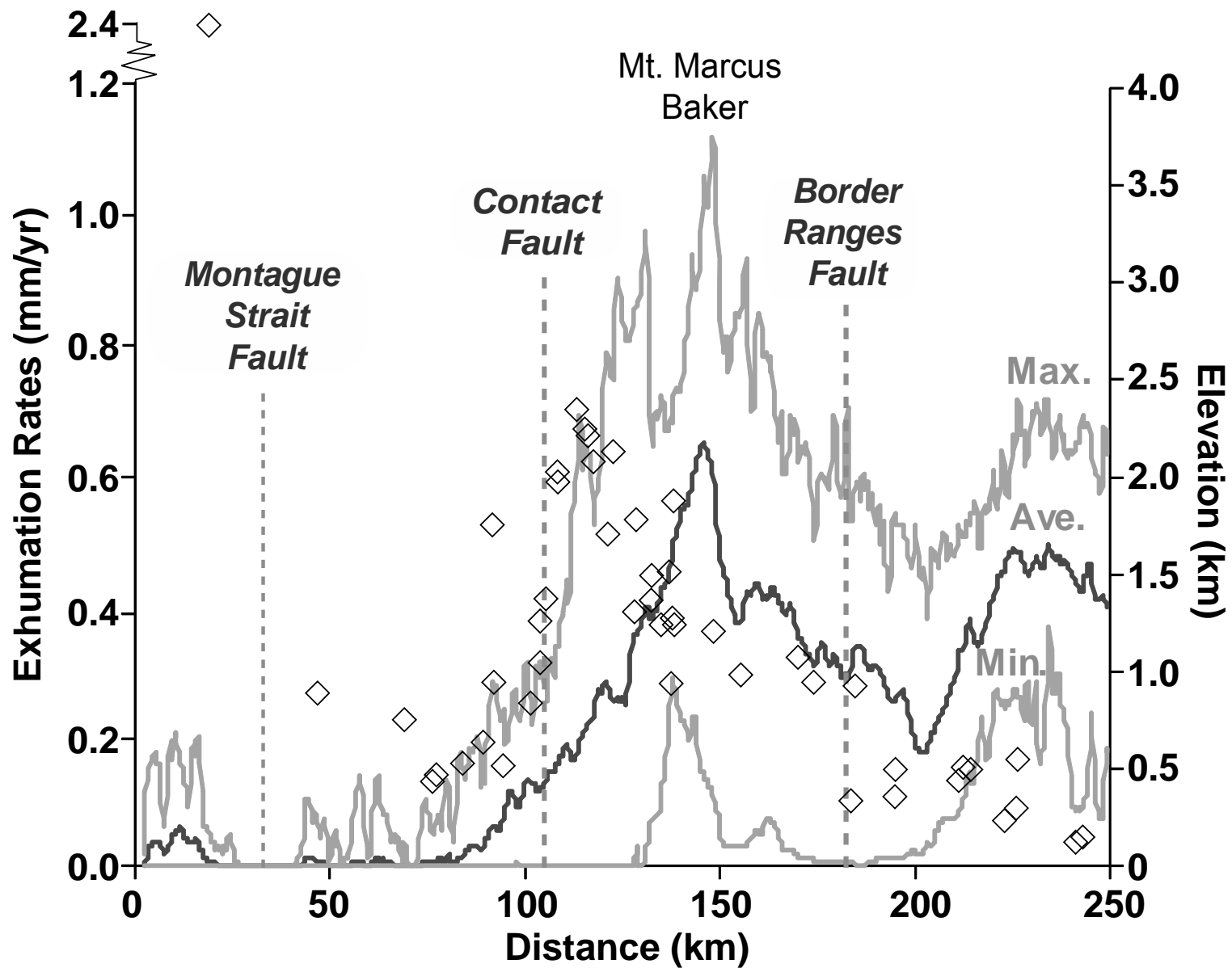
Z_{Tc} = True depth from T_c

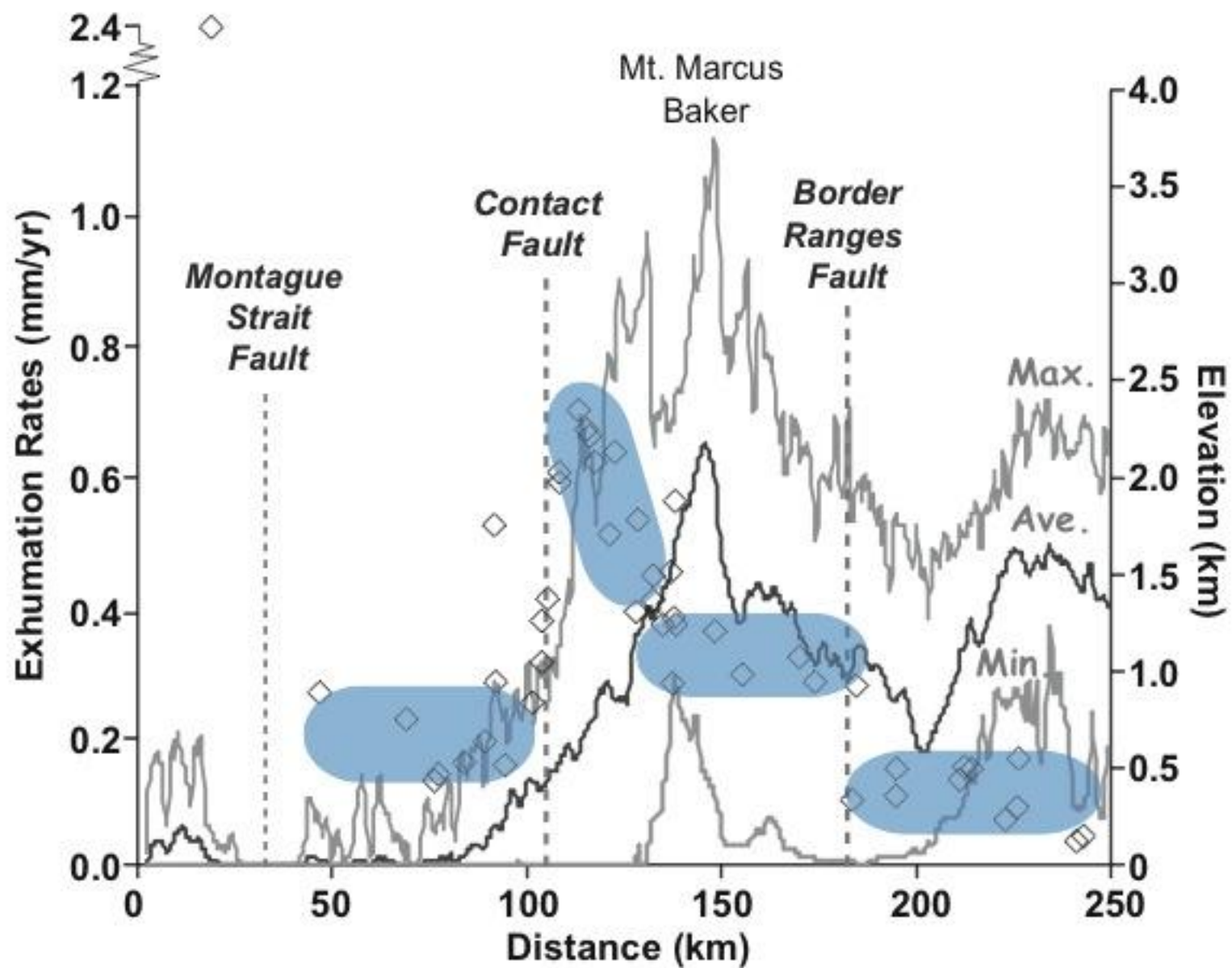




Elevation/Age Profile

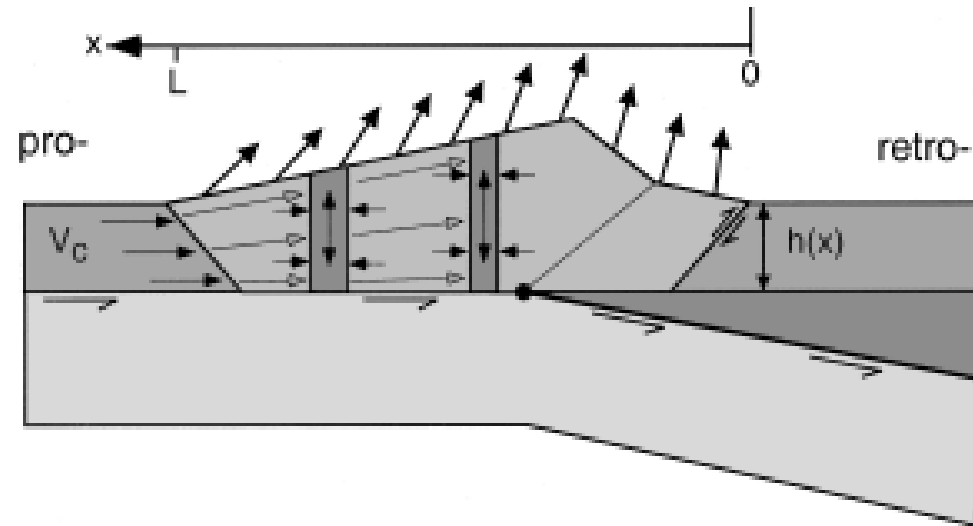




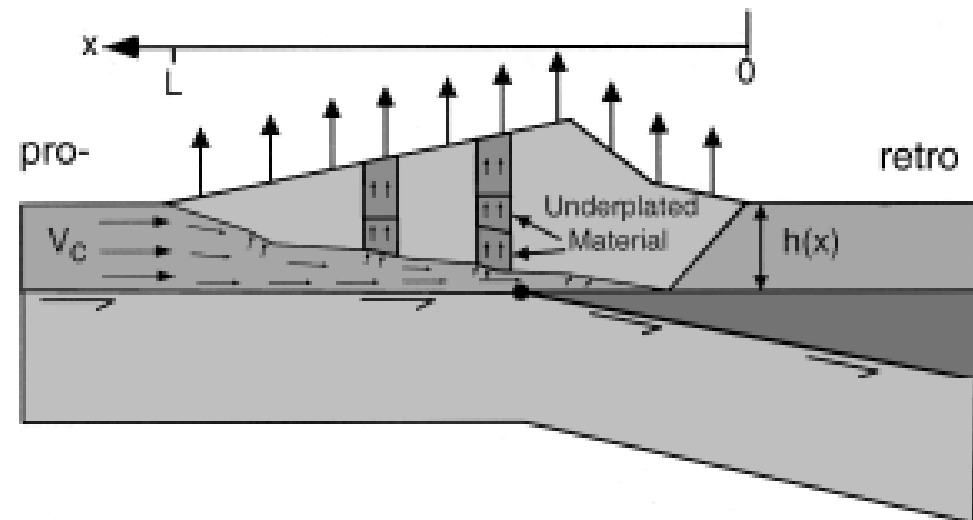


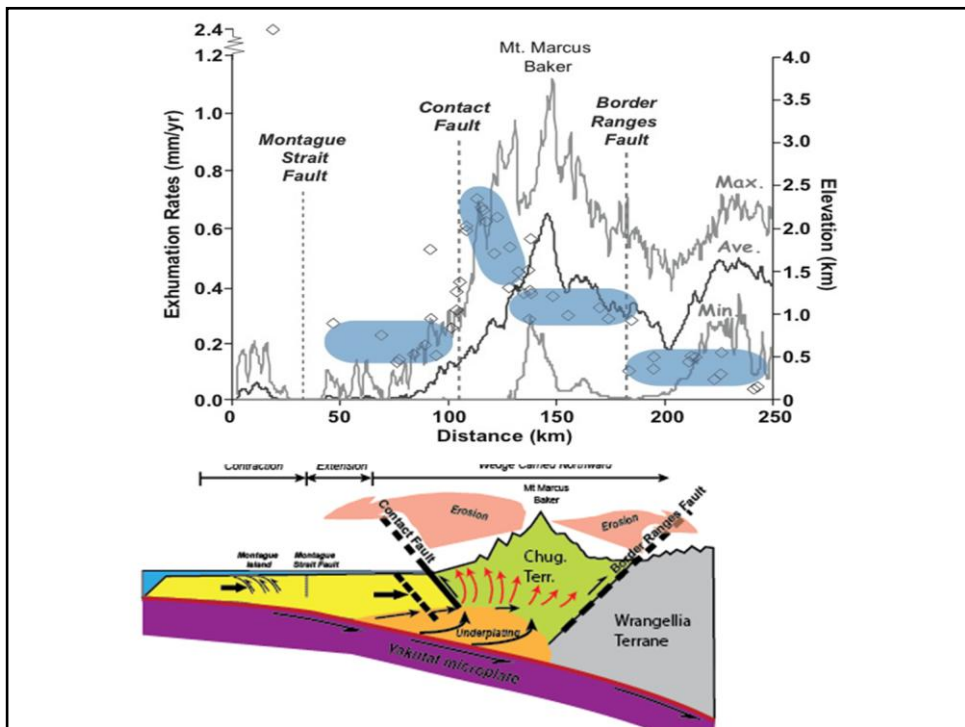
Interpretation

A. Frontal Accretion



B. Underplating

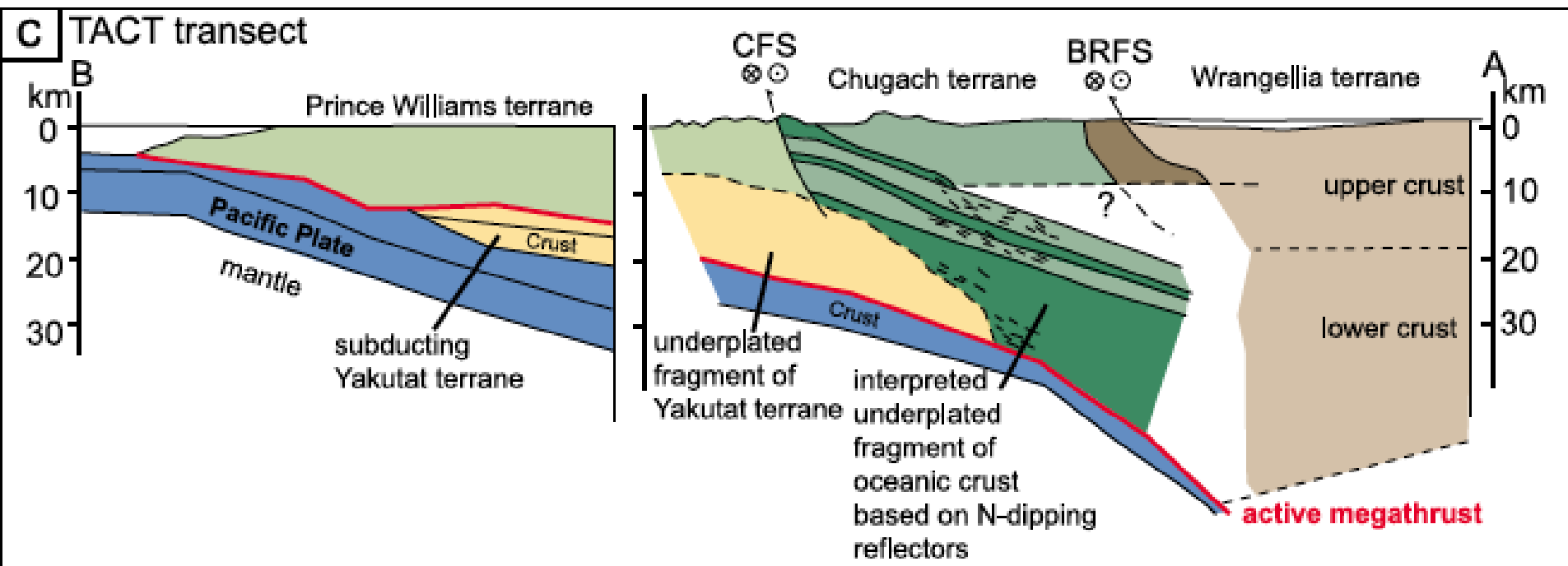




Presenter's notes: Underplating
 Modulated by climate/glaciers
 Chugach Mnt wedge driven to north – generates extension to south along Montague strait

south

north



From Fuis et al. (2008)

Summary

- Ages in the CM and NPWS decrease into syntaxial core (bulls eye in south).
- New ages fill data gap between the NPWS and BRF across CM.
- These new ages range from 10.8 to 4.7 Ma, slightly older than southern SL samples (elevation?).
- Exhumation rates relatively uniform (~ 0.4 mm/yr) across CM except adjacent to CF, where peak rates reach 0.8 mm/yr.
- Ages and rates consistent with underplating above flat slab subduction inboard of collision zone.
- Shortening and highest exhumation focused along southern wedge at the CF.

$$\text{Rate of Exhumation} = \frac{Z_{Tc}}{\text{Mean Age}}$$

$$Z_{Tc} = Z_{\text{Average}} + DZ$$

$$T_{\text{Surface}} = 0^{\circ}\text{C} \quad (\text{Péwé, 1975})$$

$$Z_{\text{Average}} = \frac{T_c - T_{\text{Surface}}}{\frac{dT}{dZ}}$$

$$\frac{dT}{dZ} = 22 \frac{^{\circ}\text{C}}{\text{km}} \quad (\text{Magoon, 1986})$$

T_c Calculated using
'CLOSURE' from
Brandon et al. (1998).

